Chemosphere 211 (2018) 226–234

Contents lists available at ScienceDirect

Chemosphere

journal homepage: www.elsevier.com/locate/chemosphere

Lignin-induced growth inhibition in soybean exposed to iron oxide nanoparticles

Tamires Letícia Cunha Lopes, Rita de Cássia Siqueira-Soares, Guilherme Henrique Gonçalves de Almeida, Gabriele Sauthier Romano de Melo, Gabriela Ellen Barreto, Dyoni Matias de Oliveira, Wanderley Dantas dos Santos, Osvaldo Ferrarese-Filho, Rogério Marchiosi*

Laboratory of Plant Biochemistry, Department of Biochemistry, University of Maringá, Maringá, PR, 87020-900, Brazil

HIGHLIGHTS

- γ-Fe_2O_3 NPs and ionic iron ($FeCl_3$) stimulated lignin formation in roots and stems.
- Lignin-induced growth inhibition was noted only in stems of plants exposed to NPs.
- Inhibition of stem growth by NPs is due to changes in lignin monomer composition.
- $FeCl_3$ and γ-Fe_2O_3 NPs act distinctly on soybean lignin metabolism.

GRAPHICAL ABSTRACT

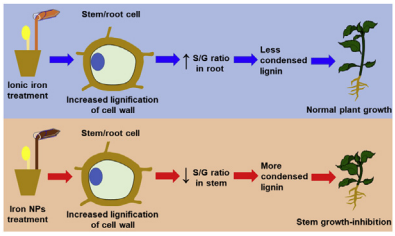

ARTICLE INFO

Article history:
Received 26 March 2018
Received in revised form
11 July 2018
Accepted 23 July 2018
Available online 26 July 2018

Handling Editor: Tamara S. Galloway

Keywords:
Lignin monomer composition
Nanopolymers
Peroxidases
Phenylalanine ammonia lyase
Phenolics
S/G ratio

ABSTRACT

Plants are occasionally exposed to environmental perturbations that limit their growth. One of these perturbations is the exposure to and interaction with various nanoparticles (NPs) that are discarded continuously into the environment. Hitherto, no study has been carried out evaluating the effects of iron oxide (γ-Fe_2O_3) NPs on soybean growth and lignin formation, as proposed herein. For comparative purposes, we also submitted soybean plants to non-nanoparticulate iron ($FeCl_3$). Exposure of the plants to γ-Fe_2O_3 NPs increased cell wall-bound peroxidase (POD) activity but decreased phenylalanine ammonia lyase (PAL) activity due, probably, to the negative feedback of accumulated phenolic compounds. In contrast, $FeCl_3$ decreased cell wall-bound POD activity. Both γ-Fe_2O_3 NPs and $FeCl_3$ increased the lignin content of roots and stems. However, significant lignin-induced growth inhibition was noted only in stems after exposure to NPs, possibly due to changes in lignin monomer composition. In this case, γ-Fe_2O_3 NPs decreased the guaiacyl monomer content of roots but increased that of stems. The high levels of monomer guaiacyl in stems resulting from the action of γ-Fe_2O_3 NPs decreased syringyl/guaiacyl ratios, generating more highly cross-linked lignin followed by the stiffening of the cell wall and growth inhibition. In contrast, $FeCl_3$ increased the contents of monomers *p*-hydroxyphenyl and syringyl in roots. The observed increase in the syringyl/guaiacyl ratio in plant roots submitted to $FeCl_3$ agrees with the lack of effect on growth, due to the formation of a less condensed lignin. In brief, we here describe that γ-Fe_2O_3 NPs and $FeCl_3$ act differently in soybean plants.

* Corresponding author.
E-mail address: marchiosi@hotmail.com (R. Marchiosi).

https://doi.org/10.1016/j.chemosphere.2018.07.143
0045-6535/

1. Introduction

Nanoparticles (NPs) are natural or man-made substances with at least one dimension smaller than 100 nm (Ju-Nam and Lead, 2008; Capaldi Arruda et al., 2015; Khan et al., 2017). According to their chemical composition, NPs can be divided into four groups: 1) inorganic NPs, 2) carbon-based NPs, 3) quantum dots, and 4) nanopolymers. NPs also exist in fused, aggregated or agglomerated forms, and can have a spherical, tubular or irregular shape (Nowack and Bucheli, 2007; Hatami et al., 2016). Their shape and reduced size bestow NPs with different chemical properties from those of their constituent elements (Brunner et al., 2006), including high chemical reactivity and surface energy, high surface area in relation to volume, and catalytic and magnetic properties (Bombin et al., 2015). These properties have allowed the wide use of NPs in industry, medicine and agriculture (Capaldi Arruda et al., 2015; Anwaar et al., 2016; Fraceto et al., 2016; Peters et al., 2016). In fact, investment in nanotechnology exceeded $224 billion in 2009, with NP production estimated to reach 58,000 tons in 2011–2020 (Bombin et al., 2015).

Industrially, NPs can be used in cosmetics as sunscreens. Titanium dioxide (TiO_2) and zinc oxide (ZnO) do not absorb visible light and block UV light, improving the efficiency of sunscreens without presenting the whitish appearance of other blockers (Ko et al., 2012). One of the most exciting applications of NPs is their use in drug loading and delivery systems. In addition to protecting the drug against premature degradation in the body, encapsulation in nanosystems helps in the direct targeting of tissues or cells, increasing drug absorption (Shaffer, 2005; Wilczewska et al., 2012). In agriculture, NPs increase productivity, improve soil quality, stimulate plant growth and provide an intelligent monitoring system for humidity, pH, temperature, and light exposure (Fraceto et al., 2016).

Iron NPs (INPs) include zero-valent iron (ZVI) and iron oxides (IONPs) such as maghemite (γ-Fe_2O_3) and magnetite (Fe_3O_4). These are useful in photocatalysis (Nie et al., 2010), gas sensors (Zhou et al., 2014), drug delivery (Bombin et al., 2015), and environmental remediation technologies (Yuvakkumar et al., 2011; Cheng et al., 2015; Vítková et al., 2018; Wan et al., 2018). Due to their wide use, the concentration of INPs in soil and water is increasing, thus necessitating the evaluation of their toxicity in living organisms. At low doses, INPs stimulate germination, root elongation, plant height, leaf biomass and chlorophyll content (Alidoust and Isoda, 2013; Rui et al., 2016; Askary et al., 2017; Hu et al., 2017; Rastogi et al., 2017). However, at relatively high doses (>100 mg L^{-1}), iron NPs reduce plant growth, root electrical conductivity, water uptake and chlorophyll accumulation, and increase reactive oxygen species (ROS) (El-Temsah and Joner, 2010; García et al., 2011; Trujillo-Reyes et al., 2014; Martínez-Fernández and Komárek, 2016). The mechanism of INPs toxicity seems to involve its aggregation and accumulation on the root surface and impairment of water and nutrient uptake (Hu et al., 2017; Zuverza-Mena et al., 2017), but its effects on plant growth deserve additional studies.

Lignification, the metabolic process of sealing a plant cell wall via lignin deposition, is a crucial stage of plant growth (Salvador et al., 2013). Lignin is an end-product of the phenylpropanoid pathway, which starts from the non-oxidative deamination of L-phenylalanine by phenylalanine ammonia-lyase (PAL) to forming *t*-cinnamate. After enzymatic chain reactions, such as hydroxylation, methoxylation, esterification and reduction, the hydroxycinnamates (*p*-coumarate, caffeate, ferulate and sinapate) are converted to their respective aldehydes, which are then further reduced to the canonical monolignols *p*-coumaryl, coniferyl and sinapyl alcohols. These last compounds are oxidatively polymerized by peroxidases (POD) to form the *p*-hydroxyphenyl (H), guaiacyl (G) and syringyl (S) monomers of lignin (Boerjan et al., 2003; Salvador et al., 2013).

Although excessive lignification is often associated with the reduction of plant growth under abiotic stresses (Cabane et al., 2012), few studies have attempted to evaluate the role of this metabolic process in the growth of plants exposed to NPs. For example, a first and recent study carried out for this purpose demonstrated that the root growth inhibition of soybean by copper oxide (CuO) NPs was correlated to increased lignification and the expression of the *PAL*, *C4H* (cinnamate 4-hydroxylase), *CAD* (cinnamyl alcohol dehydrogenase) and *POD* genes (Nair and Chung, 2014). To gain a deeper insight regarding the mechanism of toxicity of γ-Fe_2O_3 NPs, we evaluate, for the first time, their effect on soybean growth and lignin metabolism. For this, we determined the activities of PAL, soluble and cell-wall bound PODs, as well as total lignin content and its monomeric composition. We also compared the effects of iron (III) chloride ($FeCl_3$) with those observed for γ-Fe_2O_3 NPs.

2. Material and methods

2.1. Characterization of γ-Fe_2O_3 NPs

The selected γ-Fe_2O_3 NPs (particle size <50 nm (BET), surface area 50–245 m^2/g, product number 544884) were purchased from Sigma-Aldrich® (St. Louis, MO, USA). NP shape and size were determined via transmission electron microscopy (TEM). For this, 15 mg L^{-1} of γ-Fe_2O_3 NPs was suspended in distilled water and sonicated for 15 min. A drop of the NP suspension was placed in a Formvar-coated copper grid, drained through filter paper, and examined under a high-resolution transmission electron microscope (JE 1400) adjusted for an accelerating voltage of 120 kV.

2.2. General procedures

Soybean (*Glycine* max L. Merril) seeds, *cv*. BRS-232, were sanitized with 2% sodium hypochlorite for 2 min, rinsed extensively with deionized water, and distributed evenly on two Germitest® paper sheets previously moistened with deionized water. The seeds were then covered with an additional sheet of paper, and the sheets rolled and packed in plastic tubes containing a small water film to maintain moisture. The seeds were transferred to germination chambers where they remained in darkness at 25 °C for 72 h. After germination, uniform seedlings were selected, transferred into 50-mL plastic pots filled with substrate vermiculite, and watered with 25 mL of distilled water. The pots were kept in a plant growth room at 25 °C for 16 d with a light/dark photoperiod of 12/12 h and a photon flux density of 300 μmol m^{-2} s^{-1}. The plants were treated by the application to vermiculite of 25 mL of Hoagland nutrient solution (pH 6.0) containing 200–1500 mg L^{-1} of γ-Fe_2O_3 NPs, previously sonicated for 15 min. These concentrations were selected based on a survey of the literature (El-Temsah and Joner, 2010; Sheykhbaglou et al., 2010; Wang et al., 2011). Control plants were watered every other day with 25 mL of nutrient solution. For comparative purposes, additional soybean plants were treated every other day with 25 mL of Hoagland nutrient solution containing 1000 mg L^{-1} $FeCl_3$.

2.3. Plant growth parameters

After 16 d cultivation with γ-Fe_2O_3 NPs or $FeCl_3$, the soybean plants were separated into roots, stems, and leaves. Root and stem lengths and fresh weights were determined immediately. Dry weights were recorded after oven-dehydration of the plant tissues

at 70 °C for 72 h. The leaf area of the first trifolium was determined with the aid of a leaf area integrator (LI 3100, LI-COR).

2.4. Cell viability

The loss of viability of 16-d old soybean root cells was determined via Evans blue (a nonpermeating dye) staining spectrophotometric assay (Neves et al., 2012). Loss of cell viability was expressed as the absorbance of treated roots in relation to the control.

2.5. Enzymatic assays and total phenolics quantification

Soluble and cell wall-bound peroxidase (POD, EC. 1.11.1.7) activities were determined as described by dos Santos et al. (2008), and phenylalanine ammonia-lyase (PAL, EC. 4.3.1.5) activity was determined as described by Ferrarese et al. (2000). Total phenolics of roots and stems were quantified using the Folin-Ciocalteau phenol reagent (Herrig et al., 2002).

2.6. Quantification of lignin and monomer composition

The adequate acquisition of protein-free cell wall is crucial to quantifying lignin content and its monomer composition in soybean (Ferrarese et al., 2002). Dry roots and stems were subsequently washed by successive stirring and centrifugation with 50 mM phosphate buffer (pH 7.0), 1% Triton® (v:v), 1 M NaCl, distilled water and acetone. The dry matter obtained was defined as the protein-free cell wall fraction. Lignin was quantified by the acetyl bromide reaction (Moreira-Vilar et al., 2014), and alkaline nitrobenzene oxidation was used to determine lignin monomeric composition (Salvador et al., 2013).

2.7. Data analysis

The experimental design was completely randomized, with each plot represented by a 50-mL plastic pot with one plant. Data were expressed as the mean of 3–16 independent experiments ± SE. The GraphPad Prism® software package (version 5.01 GraphPad Software Inc., USA) was used for the one-way analysis of variance (Anova) to test the significance of the results. Dunnett's post-doc test was applied for experiments involving γ-Fe_2O_3 NPs, and Tukey's multiple comparison test for experiments involving γ-Fe_2O_3 NPs and $FeCl_3$; the latter results are detailed in Appendix A (Supplementary data). A significance level of $p \leq 0.05$ was considered for all analyses.

3. Results

3.1. Characterization of γ-Fe_2O_3 NPs

The TEM micrographs reveal that the γ-Fe_2O_3 NPs exhibited a spherical morphology (Fig. 1A–D). At least 80% of NPs were less than 50 nm, in agreement with the manufacturer's (Sigma-Aldrich®) specifications. The images also indicate the low homogeneity of the NPs, which varied in size from 10 to about 100 nm.

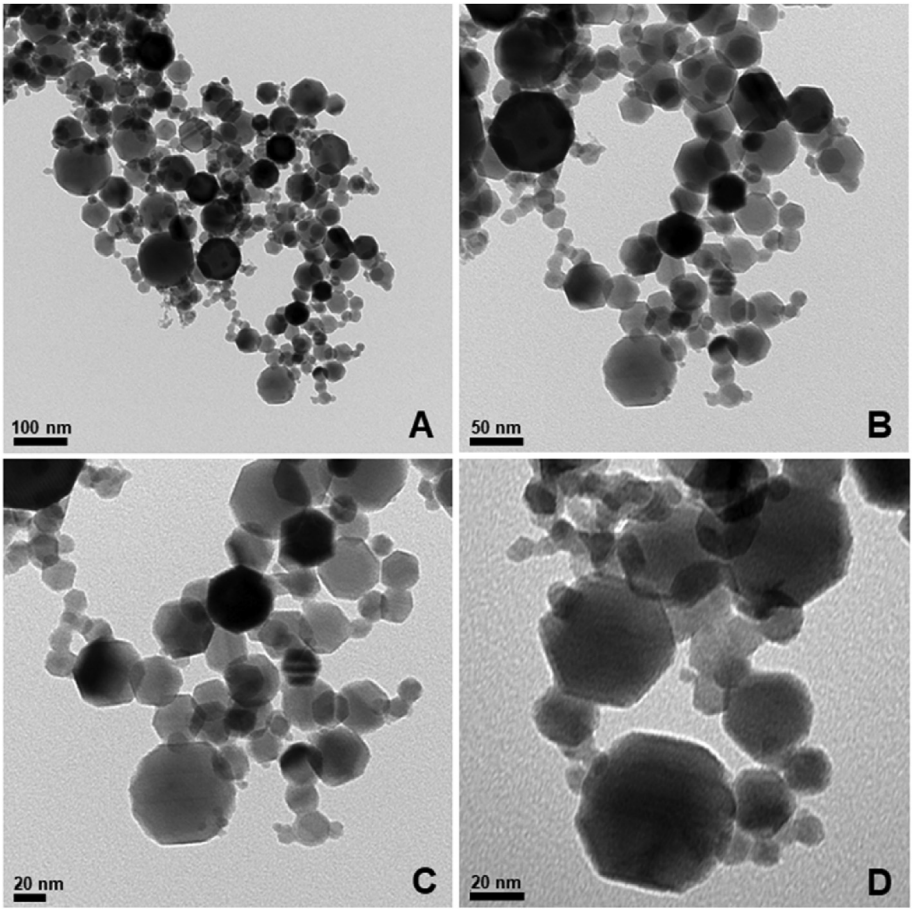

Fig. 1. TEM images of γ-Fe_2O_3 NPs, at magnifications of × 100 (A), × 200 (B), × 300 (C) and × 500 (D) thousand.

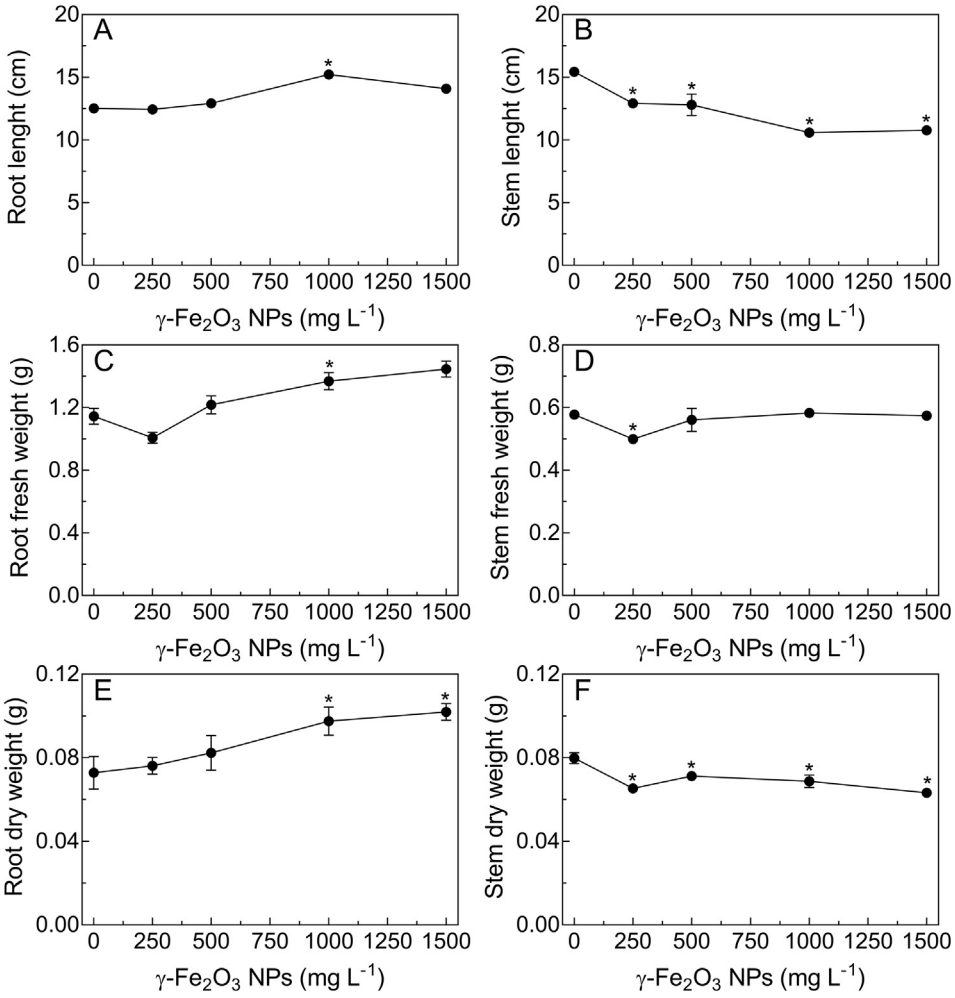

Fig. 2. Effects of γ-Fe_2O_3 NPs on soybean growth. Root length (A), stem length (B), fresh root weight (C), fresh stem weight (D), dry root weight (E) and dry stem weight (F) of soybean plants exposed to 250–1500 mg L^{-1} γ-Fe_2O_3 NPs for 16 d. *Mean (n = 4–7 ± SE) values differ statistically (Dunnett's multiple comparison test) from the control ($p \leq 0.05$).

Moreover, less than 1% of the particles were equal to 100 nm.

3.2. The γ-Fe_2O_3 NPs affected soybean growth and cell viability

The γ-Fe_2O_3 NPs increased root growth but reduced stem growth (Fig. 2). When compared to the control, root length increased by 22% only after 1000 mg L^{-1} γ-Fe_2O_3 NP exposure (Fig. 2A). After exposure to 1000 and 1500 mg L^{-1} γ-Fe_2O_3 NPs, root fresh and dry weights increased by 20% and 26% (Fig. 2C) and by 34% and 40% (Fig. 2E), respectively, in comparison to the corresponding controls. The effects of 250–1500 mg L^{-1} γ-Fe_2O_3 NPs exposure were also evident on stem length, which decreased significantly from 16% to 30%, with respect to the control (Fig. 2B). Whereas stem fresh weight was reduced by 14% at 250 mg L^{-1} γ-Fe_2O_3 NPs (Fig. 2D), dry weight was reduced by about 16% regardless of NP concentration (Fig. 2F) when compared to the corresponding control. $FeCl_3$ did not affect any growth parameter, with the exception of a 32% increase in root dry weight and a decrease of 6% in stem fresh weight, when compared to the control (Fig. S1).

The γ-Fe_2O_3 NPs did not affect leaf area (Fig. 3A). However, leaf fresh and dry weights were increased by 60% and 69% (Fig. 3B) and by 42% and 40% (Fig. 3C) after exposure to 1000 and 1500 mg L^{-1} γ-Fe_2O_3 NPs, respectively, when compared to the corresponding controls. Exposure of plants to $FeCl_3$ did not affect these parameters (Fig. S1).

The results revealed that the viability of root cells was affected by both γ-Fe_2O_3 NPs and $FeCl_3$. Uptake of Evans blue dye in roots exposed to 500–1500 mg L^{-1} γ-Fe_2O_3 NPs was, on average, 120% higher than that observed in control plants (Fig. 4). Dye uptake was also 225% higher after $FeCl_3$ exposure than in control plants, indicating a significant loss of cell viability (Fig. S2).

3.3. POD and PAL activities were altered by γ-Fe_2O_3 NPs

In roots, the activities of soluble and cell-wall bound PODs and PAL were significantly altered by γ-Fe_2O_3 NPs and $FeCl_3$. Soluble POD (Fig. 5A) and cell wall-bound POD (Fig. 5B) activities increased by 34% and 42%, and by 36% and 56%, in the 1000 and 1500 mg L^{-1} γ-Fe_2O_3 NP treatments, respectively, when compared to the corresponding controls. In contrast, PAL activities decreased in a dose-dependent manner from 22% to 60% over the exposure range of 250–1500 mg L^{-1} γ-Fe_2O_3 NPs, in comparison to the control (Fig. 5C). $FeCl_3$ exposure decreased the activities of soluble POD (by 25%), cell wall-bound POD (by 24%) and PAL (by 52%), in comparison to the controls (Fig. S3).

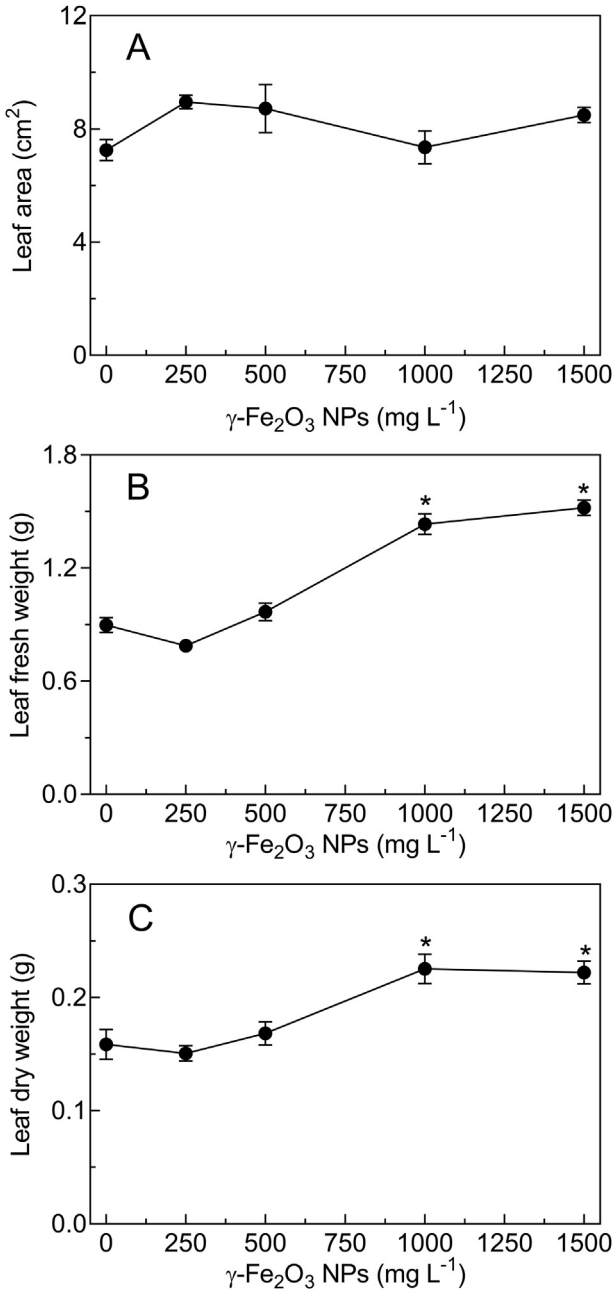

Fig. 3. Effects of γ-Fe_2O_3 NPs on soybean leaves. Leaf area (A), fresh leaf weight (B) and dry leaf weight (C) of soybean plants exposed to 250–1500 mg L^{-1} γ-Fe_2O_3 NPs for 16 d. *Mean (n = 4–7 ± SE) values differ statistically (Dunnett's multiple comparison test) from the control ($p \leq 0.05$).

3.4. The γ-Fe_2O_3 NPs increased lignin content and changed its monomeric composition

As a result of γ-Fe_2O_3 NPs exposure, root and stem lignin content was significantly different from that of the controls (Fig. 6). The exposure of soybean roots to 1000 and 1500 mg L^{-1} γ-Fe_2O_3 NPs increased lignin content by 18% and 26%, respectively, with respect to the control (Fig. 6A). At the same concentrations, γ-Fe_2O_3 NPs increased stem lignin content by 61% and 53% (Fig. 6B). Similarly, $FeCl_3$ exposure increased the lignin content of roots and stems by 28% and 53%, respectively (Fig. S4).

The obtained data revealed that γ-Fe_2O_3 NP exposure also affected the lignin monomer composition of soybean roots and stems (Fig. 6). The main change noted in roots was a reduction in G content by an average of 27% compared to the control and regardless of concentration (Fig. 6A). The γ-Fe_2O_3 NPs did not affect H and S contents, with the exception of a reduction (28%) in S monomer levels after 250 mg L^{-1} exposure. From 250 to 1500 mg L^{-1} γ-Fe_2O_3 NP exposure, stem G content was, on average, 29% higher than that observed in control plants (Fig. 6B). H monomer content increased by 38% in the 1500 mg L^{-1} γ-Fe_2O_3 NP treatment, while no change was noted in S content. $FeCl_3$ exposure increased root content of the monomers H (63%) and S (97%), and reduced that of G (32%), but had no effect on stems (Fig. S4).

Fig. 6 also summarizes the measurements recorded for lignin (referred to as the sum of H + G + S) and S/G ratios. In roots (Fig. 6A), γ-Fe_2O_3 NPs reduced H + G + S content by 39%, 28%, 34% and 25% across the 250–1500 mg L^{-1} treatment range, respectively, compared with the control. Root S/G ratios were not affected by NP exposure. In contrast, the γ-Fe_2O_3 NPs increased stem H + G + S content by an average of 22% in the 250, 1000 and 1500 mg L^{-1} treatments, when compared to the control (Fig. 6B). In addition, stem S/G ratios were reduced by around 24%–11% across the 250–1500 mg L^{-1} treatment range, with respect to the control. In turn, and only in roots, $FeCl_3$ increased the S/G ratio by 155%, without affecting any of the other parameters (Fig. S4).

Finally, phenolics contents were significantly higher in plants exposed to γ-Fe_2O_3 NPs than in the control plants (Fig. 7). In roots, γ-Fe_2O_3 NPs exposure increased phenolics content by an average of 22% across the 250–1500 mg L^{-1} treatment range (Fig. 7A). In stems, the increases in phenolics content were more evident, ranging from 84% to 124% from 250 to 1500 mg L^{-1} exposure, in comparison to the control (Fig. 7B). $FeCl_3$ increased the phenolics content of roots and stems by 12% and 158%, respectively, when compared to the corresponding controls (Fig. S5).

4. Discussion

Our findings revealed that exposure to γ-Fe_2O_3 NPs had a significant effect on the growth of soybean plants, stimulating roots and inhibiting stems (Fig. 2), and increasing the fresh and dry weights of leaves without any change in foliar area (Fig. 3). Similar stimulatory or inhibitory effects on growth have been reported elsewhere in plants submitted to NPs, in most cases in a dose-dependent manner depending on the type, concentration and exposure of the NPs, and the plant organ/tissue analyzed. For instance, γ-Fe_2O_3 NPs increased root length, plant height, biomass and values of the soil plant analysis development (SPAD) index of *Arachis hypogaea* (Rui et al., 2016). In soybean, 2000 mg L^{-1} γ-Fe_2O_3 NPs stimulated root length after 5 d of treatment, while exposure to 500–1000 mg L^{-1} increased soybean root and stem dry weights, leaf area and the SPAD index, after 14 d (Alidoust and Isoda, 2013).

It has been proposed that such increases in root length are related to the high solubility of γ-Fe_2O_3 NPs, their reduced size, which allows their uptake by the roots, and the greater availability of iron (Alidoust and Isoda, 2013; Dehner et al., 2011). On the issue of size, there is broad consensus that NPs above 20 nm do not overpass the plant cell wall (Zuverza-Mena et al., 2017). Remarkably, the uptake of 20.2 nm γ-Fe_2O_3 NPs was demonstrated in *Citrus maxima* plants, but they were not translocated from the roots to the stems (Hu et al., 2017). Although MET analysis (Fig. 1) revealed the presence of γ-Fe_2O_3 NPs with an average size of 50 nm, many were smaller than 20 nm. Considerable dispersion of NPs was evident after sonication of the suspension for 15 min, a procedure performed before the MET analyses and exposure of the soybean plants. Size, aggregation and sedimentation are important factors that should be monitored in studies involving NPs because they can alter the effectiveness of the tested concentration (Alidoust and

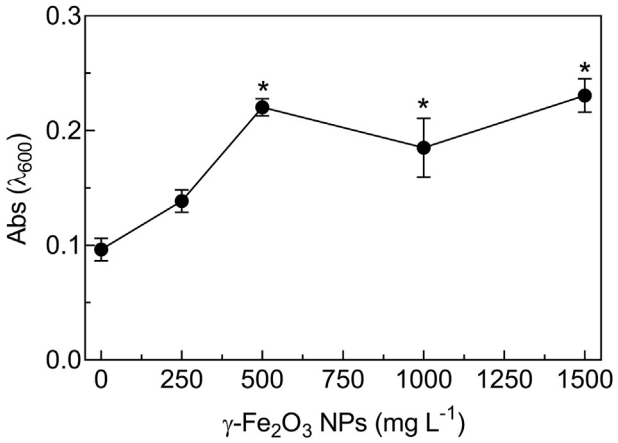

Fig. 4. Effects of γ-Fe_2O_3 NPs on cell viability. Loss of cell viability of soybean plant roots exposed to 250–1500 mg L^{-1} γ-Fe_2O_3 NPs for 16 d. Increases in absorbance values indicate a loss of cell viability with respect to the control. *Mean (n = 4–7 ± SE) values differ statistically (Dunnett's multiple comparison test) from the control ($p \leq 0.05$).

Isoda, 2013). Our findings suggest that the γ-Fe_2O_3 NPs were absorbed by the soybean roots, stimulated the growth of both roots and leaves, and increased the availability of iron. In addition, soybean plants exposed to a high concentration of ionic iron (1000 mg L^{-1} $FeCl_3$) were not affected, with the exception of an increase in root dry weight (Fig. S1). With respect to our results on soybean growth, it cannot be ruled out whether γ-Fe_2O_3 NPs influence plant growth by changing the levels of phytohormones, evidence for which has been reported previously for *Arabidopsis thaliana* (Lei et al., 2014), *Oriza sativa* (Gui et al., 2015) and *Arachis hipogaea* (Rui et al., 2016). However, this theory still requires proper investigation with regards to soybean.

Despite the stimulatory effect on roots, we also noted significant losses in cell viability after plant exposure to 500–1500 mg L^{-1} γ-Fe_2O_3 NPs (Fig. 4), and a more pronounced effect for 1000 mg L^{-1} $FeCl_3$ (Fig. S2). The IONPs reduce the hydraulic conductivity of roots and the uptake of water and nutrients due to the mechanical rupture of root membranes and cell walls (Martínez-Fernández and Komárek, 2016; Zuverza-Mena et al., 2017). This effect is due to the ability of IONPs and their aggregates to adhere to the negatively charged surface of the roots by electrostatic attraction, and connect to cation exchange sites (Trakal et al., 2015). As noted here, the reduction in cell viability was apparently not sufficient to impair water and nutrient absorption, even under $FeCl_3$ exposure (Fig. S2). Indeed, a 10-fold increase in cell viability loss is reported to be required to inhibit soybean root growth by salt stress (Neves et al., 2012). Our data also revealed that 1000 mg L^{-1} $FeCl_3$ was more toxic than γ-Fe_2O_3 NPs for soybean root cells (Fig. S2). Although iron is an essential micronutrient for the biosynthesis of heme and iron-sulfur centers, at high concentrations it can be toxic to plants (Qin et al., 2015).

One supposed mechanism of NP toxicity, including that of INPs, is the excessive generation of ROS, which induce oxidative stress in plants (Fu et al., 2014; Hatami et al., 2016). Increased activities of antioxidant enzymes, such as superoxide dismutase (SOD), peroxidase (POD) and catalase (CAT), among others, are an adaptive response of plants to scavenge ROS, aimed at reducing possible cellular damage (Soares et al., 2011). Whereas SOD is responsible for the dismutation of $O_2^{\bullet-}$ in H_2O_2, POD and CAT detoxify the latter in H_2O (Apel and Hirt, 2004). As noted, increased soluble POD activity (Fig. 5A) suggests possible oxidative stress in soybean plants exposed to γ-Fe_2O_3 NPs. This is corroborated by an increase in total

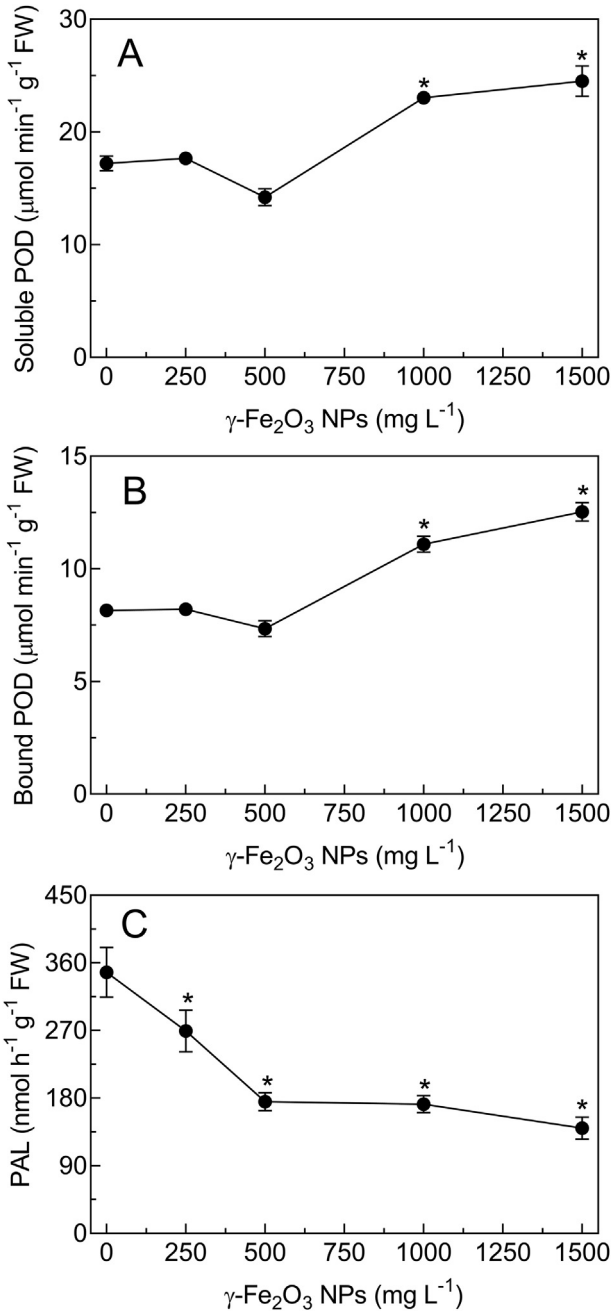

Fig. 5. Effects of γ-Fe_2O_3 NPs on enzyme activities of soybean roots. Activities of soluble peroxidase (POD) (A), cell wall-bound POD (B) and phenylalanine ammonia-lyase (PAL) (C) of soybean plants exposed to 250–1500 mg L^{-1} γ-Fe_2O_3 NPs for 16 d. *Mean (n = 4–7 ± SE) values differ statistically (Dunnett's multiple comparison test) from the control ($p \leq 0.05$).

phenolics (Fig. 7A and B), which can act as electron donors for H_2O_2 detoxification through guaiacol-type PODs (Sakihama et al., 2002; Kováčik et al., 2010). The loss of cell viability caused by the action of the γ-Fe_2O_3 NPs (Fig. 4) suggests, in principle, a slight impairment of membrane integrity due to lipid peroxidation. In agreement with our findings, increases in SOD, POD and CAT activities have been observed in both *Oriza sativa* and *Zea mays* exposed to γ-Fe_2O_3 NPs (Gui et al., 2015; Li et al., 2016). The striking finding of the present study is that γ-Fe_2O_3 NPs and ionic iron ($FeCl_3$) act distinctly on the antioxidant metabolism of soybean. In this sense, the inhibition of soluble POD activity by $FeCl_3$ (Fig. S3) indicates no oxidative stress.

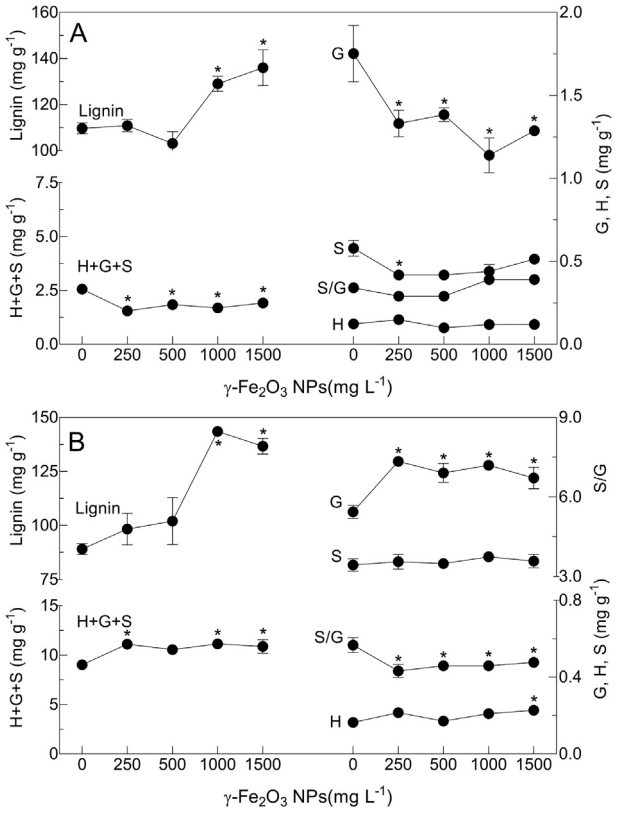

Fig. 6. Effects of γ-Fe_2O_3 NPs on soybean lignin content and monomeric composition. Contents of lignin, guaiacyl (G), syringyl (S), *p*-hydroxyphenyl (H), H + G + S and S/G ratios in roots (A) and stems (B) of soybean plants exposed to 250–1500 mg L^{-1} γ-Fe_2O_3 NPs for 16 d. *Mean (n = 3–7 ± SE) values differ statistically (Dunnett's multiple comparison test) from the control ($p \leq 0.05$).

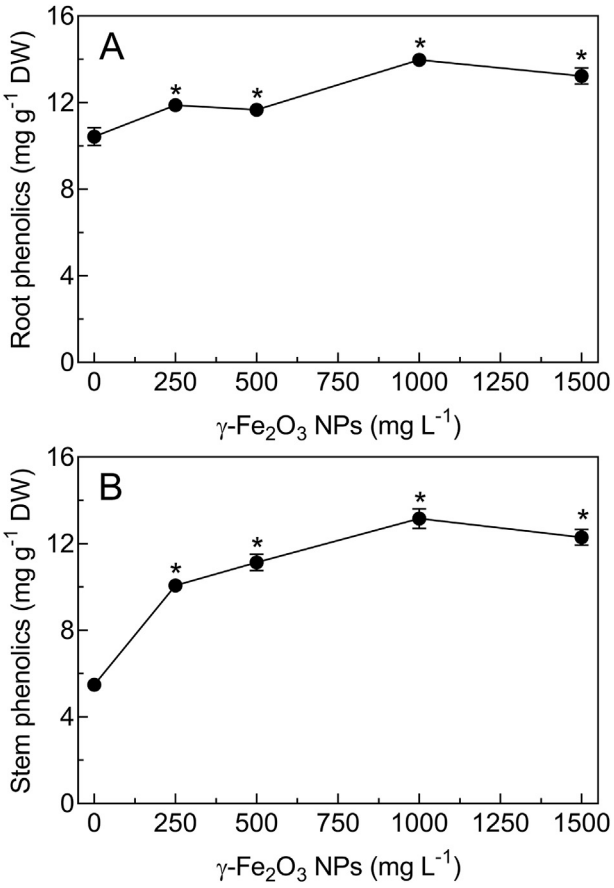

Fig. 7. Effects of γ-Fe_2O_3 NPs on soybean total phenolics content. Content of total phenolics in the roots (A) and stems (B) of soybean plants exposed to 250–1500 mg L^{-1} γ-Fe_2O_3 NPs for 16 d. *Mean (n = 4–7 ± SE) values differ statistically (Dunnett's multiple comparison test) from the control ($p \leq 0.05$).

Another fact observed here is that the γ-Fe_2O_3 NPs affected soybean lignification in the form of a significant increase in the lignin contents of roots (Fig. 6A) and stems (Fig. 6B). Increased lignification in plants is considered a defense mechanism against abiotic stress, with allelochemicals such as cinnamic acid and derivatives reported to impair soybean root growth due to the associated premature cell wall lignification (dos Santos et al., 2008; Zanardo et al., 2009; Bubna et al., 2011; Salvador et al., 2013). When compared to the corresponding controls, γ-Fe_2O_3 NPs exposure here increased lignin content in stems (Fig. 6B) to a greater degree than in roots (Fig. 6A). Thus, because stress-induced lignification limits cell expansion, nutrient uptake and plant growth, this finding could explain the stem growth-inhibition caused by the γ-Fe_2O_3 NPs (Fig. 2B). In turn, the observed root lignification seemed to be insufficient to limit longitudinal growth (Fig. 2A), although it did contribute to an increase in fresh and dry weights (Fig. 2C, E). Increased lignification has been reported in several plant species submitted to silver, silicon, copper oxide and zinc oxide NPs (Asgari et al., 2018; Bernard et al., 2015; Nair and Chung, 2015; Nazaralian et al., 2017; Prakash and Chung, 2016). For example, silicon NPs increased xylem cell wall lignification without changing the growth of *Avena sativa* and *Trigonella feonum-graecum* (Nazaralian et al., 2017; Asgari et al., 2018). In agreement with our findings, lignin induced growth inhibition was observed in *Brassica juncea* and *Triticum aestivum* exposed to copper oxide and zinc oxide NPs, respectively (Nair and Chung, 2015; Prakash and Chung, 2016).

A high lignin content may be related to the increased activity of PAL, which plays a key role in the phenylpropanoid pathway (Boerjan et al., 2003; Lima et al., 2013; Salvador et al., 2013). As an example, silicon NPs increased the expression and activity of PAL as well as lignin content in *Avena sativa* and *Trigonella foenum-graecum* (Nazaralian et al., 2017; Asgari et al., 2018). However, here PAL activity decreased due to the action of the γ-Fe_2O_3 NPs (Fig. 5C), in contrast to root lignin content (Fig. 6A). Similar behavior has been observed in soybean roots submitted to cinnamic and benzoic acids derivatives, which inhibit PAL activity both *in vitro* (Sato et al., 1982) and *in vivo* (Bubna et al., 2011). So, one plausible explanation for PAL inhibition by γ-Fe_2O_3 NPs (Fig. 7A) could be a negative feedback caused by phenolic compound accumulation in tissues (Dixon and Paiva, 1995; Zanardo et al., 2009).

The present study also revealed a stimulatory effect of γ-Fe_2O_3 NPs on cell wall-bound POD activities (Fig. 5B). To polymerize monolignols into lignin, this enzyme uses H_2O_2, which, at the reduced level, can indirectly down-regulate PAL activity (Zanardo et al., 2009; Bubna et al., 2011). In agreement with our results, increased lignin content in soybean exposed to copper oxide (CuO) NPs has been related to the reduced growth of roots and stems, and increased levels of transcripts for anionic and cationic PODs (Nair and Chung, 2014). In addition, increased POD activity and lignin content were noted in roots of *Triticum aestivum* exposed to zinc oxide NPs (Prakash and Chung, 2016).

Another interesting finding is that γ-Fe_2O_3 NPs exposure altered lignin monomer composition (Fig. 6). In this sense, γ-Fe_2O_3 NPs and $FeCl_3$ appear to act oppositely, since the monomeric profiles of roots and stems were clearly different. In stems, the most evident change caused by γ-Fe_2O_3 NPs exposure was an increased G monomer

content, which resulted in a significant increase in H + G + S values and a low S/G ratio (Fig. 6B). The S/G ratio predicts the degree and nature of lignin cross-linking and, in the current case, indicates a more condensed and rigid polymer (Cesarino et al., 2012). Therefore, our findings suggest that a highly cross-linked lignin polymer can contribute to reduced cell wall expansion and the longitudinal growth of stems. In contrast, γ-Fe_2O_3 NPs significantly decreased root G unit numbers (Fig. 6A) and, as a result, decreased root H + G + S content, a possible indication of less condensed lignin. This fact may explain the absence of any strong effect on root growth (Fig. 2A) in comparison to that observed in stems (Fig. 2B). The absence of any effect of $FeCl_3$ on root growth is likely related to the formation of less cross-linked lignin, since a relevant increase in the S/G ratio (0.87) was also observed in this treatment (Fig. S1).

5. Conclusion

The most interesting findings of the current work indicate that the stem growth-inhibition observed in soybean plants exposed to γ-Fe_2O_3 NPs can be explained not only by increased lignin production, but also by changes in monomer composition. The high G monomer content in stems lowered the S/G ratio, generating a more highly cross-linked lignin with subsequent stiffening of the cell wall and inhibition of growth. In addition, the effects caused by the γ-Fe_2O_3 NPs diverged from those caused by the metal of the same valence ($FeCl_3$), evidencing that the two acts differently in soybean.

Conflicts of interest

The authors declare that the research was conducted in the absence of any commercial or financial relationships that could be construed as a potential conflict of interest.

Acknowledgements

This work was supported by grants from The National Council for Scientific and Technological Development - CNPq (nº3052018/2013-1). Osvaldo Ferrarese-Filho is research fellow of CNPq. Tamires Letícia Cunha Lopes was the recipient of a CNPq fellowship. The authors thank Andressa Pelozo by the aid provided in the microscopy analyzes.

Appendix A. Supplementary data

Supplementary data related to this article can be found at https://doi.org/10.1016/j.chemosphere.2018.07.143.

References

Alidoust, D., Isoda, A., 2013. Effect of γ-Fe_2O_3 nanoparticles on photosynthetic characteristic of soybean (*Glycine max* (L.) Merr.): foliar spray versus soil amendment. Acta Physiol. Plant. 35, 3365–3375. https://doi.org/10.1007/s11738-013-1369-8.

Anwaar, S., Maqbool, Q., Jabeen, N., Nazar, M., Abbas, F., Nawaz, B., Hussain, T., Hussain, S.Z., 2016. The effect of green synthesized CuO nanoparticles on callogenesis and regeneration of *Oryza sativa* L. Front. Plant Sci. 7, 1–9. https://doi.org/10.3389/fpls.2016.01330.

Apel, K., Hirt, H., 2004. Reactive oxygen species: metabolism, oxidative stress, and signal transduction. Annu. Rev. Plant Biol. 55, 373–399. https://doi.org/10.1146/annurev.arplant.55.031903.141701.

Asgari, F., Majd, A., Jonoubi, P., Najafi, F., 2018. Effects of silicon nanoparticles on molecular, chemical, structural and ultrastructural characteristics of oat (*Avena sativa* L.). Plant Physiol. Biochem. 127, 152–160. https://doi.org/10.1016/j.plaphy.2018.03.021.

Askary, M., Talebi, S.M., Amini, F., Bangan, A.D.B., 2017. Effects of iron nanoparticles on *Mentha piperita* L. under salinity stress. Biologija 63, 65–75.

Bernard, F., Navab Moghadam, N., Mirzajani, F., 2015. The effect of colloidal silver nanoparticles on the level of lignification and hyperhydricity syndrome in *Thymus daenensis* vitro shoots: a possible involvement of bonded polyamines. Vitro Cell Dev. Biol. Plant 51, 546–553. https://doi.org/10.1007/s11627-015-9700-2.

Boerjan, W., Ralph, J., Baucher, M., 2003. Lignin biosynthesis. Annu. Rev. Plant Biol. 54, 519–546. https://doi.org/10.1146/annurev.arplant.54.031902.134938.

Bombin, S., LeFebvre, M., Sherwood, J., Xu, Y., Bao, Y., Ramonell, K.M., 2015. Developmental and reproductive effects of iron oxide nanoparticles in *Arabidopsis thaliana*. Int. J. Mol. Sci. 16, 24174–24193. https://doi.org/10.3390/ijms161024174.

Brunner, T.J., Wick, P., Manser, P., Spohn, P., Grass, R.N., Limbach, L.K., Bruinink, A., Stark, W.J., 2006. In vitro cytotoxicity of oxide nanoparticles: comparison to asbestos, silica, and the effect of particle solubility. Environ. Sci. Technol. 40, 4374–4381. https://doi.org/10.1021/es052069i.

Bubna, G.A., Lima, R.B., Zanardo, D.Y.L., dos Santos, W.D., Ferrarese, M. de L.L., Ferrarese-Filho, O., 2011. Exogenous caffeic acid inhibits the growth and enhances the lignification of the roots of soybean (*Glycine max*). J. Plant Physiol. 168, 1627–1633. https://doi.org/10.1016/j.jplph.2011.03.005.

Cabane, M., Afif, D., Hawkins, S., 2012. Lignins and abiotic stresses. In: Jouanin, L., Lapierre, C. (Eds.), Lignins: Biosynthesis, Biodegradation and Bioengineering. San Diego, pp. 219–261.

Capaldi Arruda, S.C., Diniz Silva, A.L., Moretto Galazzi, R., Antunes Azevedo, R., Zezzi Arruda, M.A., 2015. Nanoparticles applied to plant science: a review. Talanta 131, 693–705. https://doi.org/10.1016/j.talanta.2014.08.050.

Cesarino, I., Araújo, P., Domingues Júnior, A.P., Mazzafera, P., 2012. An overview of lignin metabolism and its effect on biomass recalcitrance. Braz. J. Bot. 35, 303–311. https://doi.org/10.1590/S0100-84042012000400003.

Cheng, W., Xu, J., Wang, Y., Wu, F., Xu, X., Li, J., 2015. Dispersion-precipitation synthesis of nanosized magnetic iron oxide for efficient removal of arsenite in water. J. Colloid Interface Sci. 445, 93–101. https://doi.org/10.1016/j.jcis.2014.12.082.

Dehner, C.A., Barton, L., Maurice, P.A., Dubois, J.L., 2011. Size-dependent bioavailability of hematite (α-Fe_2O_3) nanoparticles to a common aerobic bacterium. Environ. Sci. Technol. 977–983. https://doi.org/10.1007/s10973-009-0475-8.

Dixon, R.A., Paiva, N.L., 1995. Stress-induced phenylpropanoid metabolism. Plant Cell 7, 1085. https://doi.org/10.2307/3870059.

Dos Santos, W.D., Ferrarese, M.L.L., Nakamura, C.V., Mourão, K.S.M., Mangolin, C.A., Ferrarese-Filho, O., 2008. Soybean (*Glycine max*) root lignification induced by ferulic acid. The possible mode of action. J. Chem. Ecol. 34, 1230–1241. https://doi.org/10.1007/s10886-008-9522-3.

El-Temsah, Y.S., Joner, E.J., 2010. Impact of Fe and Ag nanoparticles on seed germination and differences in bioavailability during exposure in aqueous suspension and soil. Environ. Toxicol. 27, 42–49. https://doi.org/10.1002/tox.

Ferrarese, M.L.L., Rodrigues, J.D., Ferrarese-Filho, O., 2000. Phenylalanine ammonia-lyase activity in soybean roots extract measured by reverse-phase high performance liquid chromatography. Plant Biol. 2, 152–153. https://doi.org/10.1055/s-2000-9162.

Ferrarese, M.L.L., Zottis, A., Ferrarese-Filho, O., 2002. Protein-free lignin quantification in soybean (*Glycine max*) roots. Biologia 57, 541–543.

Fraceto, L.F., Grillo, R., de Medeiros, G.A., Scognamiglio, V., Rea, G., Bartolucci, C., 2016. Nanotechnology in Agriculture: which innovation potential does it have? Front. Environ. Sci. 4, 1–5. https://doi.org/10.3389/fenvs.2016.00020.

Fu, P.P., Xia, Q., Hwang, H.M., Ray, P.C., Yu, H., 2014. Mechanisms of nanotoxicity: generation of reactive oxygen species. J. Food Drug Anal. 22, 64–75. https://doi.org/10.1016/j.jfda.2014.01.005.

García, A., Espinosa, R., Delgado, L., Casals, E., González, E., Puntes, V., Barata, C., Font, X., Sánchez, A., 2011. Acute toxicity of cerium oxide, titanium oxide and iron oxide nanoparticles using standardized tests. Desalination 269, 136–141. https://doi.org/10.1016/j.desal.2010.10.052.

Gui, X., Deng, Y., Rui, Y., Gao, B., Luo, W., Chen, S., Van Nhan, L., Li, X., Liu, S., Han, Y., Liu, L., Xing, B., 2015. Response difference of transgenic and conventional rice (*Oryza sativa*) to nanoparticles (γ-Fe_2O_3). Environ. Sci. Pollut. Res. 22, 17716–17723. https://doi.org/10.1007/s11356-015-4976-7.

Hatami, M., Kariman, K., Ghorbanpour, M., 2016. Engineered nanomaterial-mediated changes in the metabolism of terrestrial plants. Sci. Total Environ. 571, 275–291. https://doi.org/10.1016/j.scitotenv.2016.07.184.

Herrig, V., Ferrarese, M.L.L., Suzuki, L.S., Rodrigues, J.D., Ferrarese-Filho, O., 2002. Peroxidase and phenylalanine ammonia-lyase activities, phenolic acid contents, and allelochemicals-inhibited root growth of soybean. Biol. Res. 35, 59–66.

Hu, J., Guo, H., Li, J., Gan, Q., Wang, Y., Xing, B., 2017. Comparative impacts of iron oxide nanoparticles and ferric ions on the growth of *Citrus maxima*. Environ. Pollut. 221, 199–208. https://doi.org/10.1016/j.envpol.2016.11.064.

Ju-Nam, Y., Lead, J.R., 2008. Manufactured nanoparticles: an overview of their chemistry, interactions and potential environmental implications. Sci. Total Environ. 400, 396–414. https://doi.org/10.1016/j.scitotenv.2008.06.042.

Khan, M.N., Mobin, M., Abbas, Z.K., AlMutairi, K.A., Siddiqui, Z.H., 2017. Role of nanomaterials in plants under challenging environments. Plant Physiol. Biochem. 110, 194–209. https://doi.org/10.1016/j.plaphy.2016.05.038.

Ko, H.H., Chen, H.T., Yen, F.L., Lu, W.C., Kuo, C.W., Wang, M.C., 2012. Preparation of TiO_2 nanocrystallite powders coated with 9 mol% ZnO for cosmetic applications in sunscreens. Int. J. Mol. Sci. 13, 1658–1669. https://doi.org/10.3390/ijms13021658.

Kováčik, J., Grúz, J., Klejdus, B., Štork, F., Marchiosi, R., Ferrarese-Filho, O., 2010. Lignification and related parameters in copper-exposed *Matricaria chamomilla* roots: role of H_2O_2 and NO in this process. Plant Sci. 179, 383–389. https://doi.org/10.1016/j.plantsci.2010.06.014.

Lei, G.J., Zhu, X.F., Wang, Z.W., Dong, F., Dong, N.Y., Zheng, S.J., 2014. Abscisic acid alleviates iron deficiency by promoting root iron reutilization and transport from root to shoot in arabidopsis. Plant Cell Environ. 37, 852–863. https://doi.org/10.1111/pce.12203.

Li, J., Hu, J., Ma, C., Wang, Y., Wu, C., Huang, J., Xing, B., 2016. Uptake, translocation and physiological effects of magnetic iron oxide (γ-Fe_2O_3) nanoparticles in corn (*Zea mays* L.). Chemosphere 159, 326–334. https://doi.org/10.1016/j.chemosphere.2016.05.083.

Lima, R.B., Salvador, V.H., Dos Santos, W.D., Bubna, G.A., Finger-Teixeira, A., Soares, A.R., Marchiosi, R., Ferrarese, M.D.L.L., Ferrarese-Filho, O., 2013. Enhanced lignin monomer production caused by cinnamic acid and its hydroxylated derivatives inhibits soybean root growth. PLoS One 8, 1–8. https://doi.org/10.1371/journal.pone.0080542.

Martínez-Fernández, D., Komárek, M., 2016. Comparative effects of nanoscale zero-valent iron (nZVI) and Fe_2O_3 nanoparticles on root hydraulic conductivity of *Solanum lycopersicum* L. Environ. Exp. Bot. 131, 128–136. https://doi.org/10.1016/j.envexpbot.2016.07.010.

Moreira-Vilar, F.C., Siqueira-Soares, R.D.C., Finger-Teixeira, A., De Oliveira, D.M., Ferro, A.P., Da Rocha, G.J., Ferrarese, M.D.L.L., Dos Santos, W.D., Ferrarese-Filho, O., 2014. The acetyl bromide method is faster, simpler and presents best recovery of lignin in different herbaceous tissues than klason and thioglycolic acid methods. PLoS One 9. https://doi.org/10.1371/journal.pone.0110000.

Nair, P.M.G., Chung, I.M., 2015. Study on the correlation between copper oxide nanoparticles induced growth suppression and enhanced lignification in Indian mustard (*Brassica juncea* L.). Ecotoxicol. Environ. Saf. 113, 302–313. https://doi.org/10.1016/j.ecoenv.2014.12.013.

Nair, P.M.G., Chung, I.M., 2014. A mechanistic study on the toxic effect of copper oxide nanoparticles in soybean (*Glycine max* L.) root development and lignification of root cells. Biol. Trace Elem. Res. 162, 342–352. https://doi.org/10.1007/s12011-014-0106-5.

Nazaralian, S., Majd, A., Irian, S., Najafi, F., Ghahremaninejad, F., Landberg, T., Greger, M., 2017. Comparison of silicon nanoparticles and silicate treatments in fenugreek. Plant Physiol. Biochem. 115, 25–33. https://doi.org/10.1016/j.plaphy.2017.03.009.

Neves, G.Y.S., de Lourdes Lucio Ferrarese, M., Marchiosi, R., de Cássia Siqueira-Soares, R., Ferrarese-Filho, O., 2012. Effects of calcium on lignification related parameters in sodium chloride-stressed soybean roots. J. Plant Nutr. 35, 1657–1670. https://doi.org/10.1080/01904167.2012.698347.

Nie, Y., Hu, C., Zhou, L., Qu, J., Wei, Q., Wang, D., 2010. Degradation characteristics of humic acid over iron oxides/FeO core-shell nanoparticles with UVA/H_2O_2. J. Hazard Mater. 173, 474–479. https://doi.org/10.1016/j.jhazmat.2009.08.109.

Nowack, B., Bucheli, T.D., 2007. Occurrence, behavior and effects of nanoparticles in the environment. Environ. Pollut. 150, 5–22. https://doi.org/10.1016/j.envpol.2007.06.006.

Peters, R.J.B., Bouwmeester, H., Gottardo, S., Amenta, V., Arena, M., Brandhoff, P., Marvin, H.J.P., Mech, A., Moniz, F.B., Pesudo, L.Q., Rauscher, H., Schoonjans, R., Undas, A.K., Vettori, M.V., Weigel, S., Aschberger, K., 2016. Nanomaterials for products and application in agriculture, feed and food. Trends Food Sci. Technol. 54, 155–164. https://doi.org/10.1016/j.tifs.2016.06.008.

Prakash, M.G., Chung, I.M., 2016. Determination of zinc oxide nanoparticles toxicity in root growth in wheat (*Triticum aestivum* L.) seedlings. Acta Biol. Hung. 67, 286–296. https://doi.org/10.1556/018.67.2016.3.6.

Qin, L., Wang, M., Zuo, J., Feng, X., Liang, X., Wu, Z., Ye, H., 2015. Cytosolic BolA plays a repressive role in the tolerance against excess iron and MV-induced oxidative stress in plants. PLoS One 10, 1–20. https://doi.org/10.1371/journal.pone.0124887.

Rastogi, A., Zivcak, M., Sytar, O., Kalaji, H.M., He, X., Mbarki, S., Brestic, M., 2017. Impact of metal and metal oxide nanoparticles on plant: a critical review. Front. Chem. 5, 1–16. https://doi.org/10.3389/fchem.2017.00078.

Rui, M., Ma, C., Hao, Y., Guo, J., Rui, Y., Tang, X., Zhao, Q., Fan, X., Zhang, Z., Hou, T., Zhu, S., 2016. Iron oxide nanoparticles as a potential iron fertilizer for peanut (*Arachis hypogaea*). Front. Plant Sci. 7, 1–10. https://doi.org/10.3389/fpls.2016.00815.

Sakihama, Y., Cohen, M.F., Grace, S.C., Yamasaki, H., 2002. Plant phenolic antioxidant and prooxidant activities: phenolics-induced oxidative damage mediated by metals in plants. Toxicology 177, 67–80. https://doi.org/10.1016/S0300-483X(02)00196-8.

Salvador, V.H., Lima, R.B., dos Santos, W.D., Soares, A.R., Böhm, P.A.F., Marchiosi, R., Ferrarese, M., de, L.L., Ferrarese-Filho, O., 2013. Cinnamic acid increases lignin production and inhibits soybean root growth. PLoS One 8, 1–10. https://doi.org/10.1371/journal.pone.0069105.

Sato, T., Kiuchi, F., Sankawa, U., 1982. Inhibition of phenylalanine ammonia-lyase by cinnamic acid derivatives and related compounds. Phytochemistry 21, 845–850.

Shaffer, C., 2005. Nanomedicine transforms drug delivery. Drug Discov. Today 10, 1581–1582.

Sheykhbaglou, R., Sedghi, M., Tajbakhsh Shishevan, M., Sharifi, R.S., 2010. Effects of nano-iron oxide particles on agronomic traits of soybean. Not. Sci. Biol. 2, 112–113. https://doi.org/10.1039/b805998e.

Soares, A.R., de Ferrarese, M.L.L., de Siqueira-Soares, R.C., Marchiosi, R., Finger-Teixeira, A., Ferrarese-Filho, O., 2011. The allelochemical L-DOPA increases melanin production and reduces reactive oxygen species in soybean roots. J. Chem. Ecol. 37, 891–898. https://doi.org/10.1007/s10886-011-9988-2.

Trakal, L., Martínez-Fernández, D., Vítková, M., Komárek, M., 2015. Phytoextraction of metals: modeling root metal uptake and associated processes. In: Ansari, A.A., Gill, S.S., Gill, R., Lanza, G.R., Lee, N. (Eds.), Phytoremediation: Management of Environmental Contaminants. Springer, pp. 69–83.

Trujillo-Reyes, J., Majumdar, S., Botez, C.E., Peralta-Videa, J.R., Gardea-Torresdey, J.L., 2014. Exposure studies of core-shell Fe/Fe_3O_4 and Cu/CuO NPs to lettuce (*Lactuca sativa*) plants: are they a potential physiological and nutritional hazard? J. Hazard Mater. 267, 255–263. https://doi.org/10.1016/j.jhazmat.2013.11.067.

Vítková, M., Puschenreiter, M., Komárek, M., 2018. Effect of nano zero-valent iron application on As, Cd, Pb, and Zn availability in the rhizosphere of metal(loid) contaminated soils. Chemosphere 200, 217–226. https://doi.org/10.1016/j.chemosphere.2018.02.118.

Wan, J., Jiang, X., Zhang, T.C., Hu, J., Richter-Egger, D., Feng, X., Zhou, A., Tao, T., 2018. The activated iron system for phosphorus recovery in aqueous environments. Chemosphere 196, 153–160. https://doi.org/10.1016/j.chemosphere.2017.12.140.

Wang, H., Kou, X., Pei, Z., Xiao, J.Q., Shan, X., Xing, B., 2011. Physiological effects of magnetite (Fe_3O_4) nanoparticles on perennial ryegrass (*Lolium perenne* L.) and pumpkin (*Cucurbita mixta*) plants. Nanotoxicology 5, 30–42.

Wilczewska, A.Z., Niemirowicz, K., Markiewicz, K.H., Car, H., 2012. Nanoparticles as drug delivery systems. Pharmacol. Rep. 64, 1020–1037. https://doi.org/10.1016/S1734-1140(12)70901-5.

Yuvakkumar, R., Elango, V., Rajendran, V., Kannan, N., 2011. Preparation and characterization of zero valent iron nanoparticles. Dig. J. Nanomater. Biostruct. 6, 1771–1776. https://doi.org/10.1007/s10661-011-2213-5.

Zanardo, D.I.L., Lima, R.B., Ferrarese, M.deL.L., Bubna, G.A., Ferrarese-Filho, O., 2009. Soybean root growth inhibition and lignification induced by *p*-coumaric acid. Environ. Exp. Bot. 66, 25–30. https://doi.org/10.1016/j.envexpbot.2008.12.014.

Zhou, X., Wang, C., Feng, W., Sun, P., Li, X., Lu, G., 2014. Hollow α-Fe_2O_3 quasi-cubic structures: hydrothermal synthesis and gas sensing properties. Mater. Lett. 120, 5–8. https://doi.org/10.1016/j.matlet.2014.01.047.

Zuverza-Mena, N., Martínez-Fernández, D., Du, W., Hernandez-Viezcas, J.A., Bonilla-Bird, N., López-Moreno, M.L., Komárek, M., Peralta-Videa, J.R., Gardea-Torresdey, J.L., 2017. Exposure of engineered nanomaterials to plants: insights into the physiological and biochemical responses-A review. Plant Physiol. Biochem. 110, 236–264. https://doi.org/10.1016/j.plaphy.2016.05.037.